Applied Thermal Engineering 72 (2014) 2–9

Contents lists available at ScienceDirect

Applied Thermal Engineering

journal homepage: www.elsevier.com/locate/apthermeng

Effective structure of aerogels and decomposed contributions of its thermal conductivity

Dan Dan, Hu Zhang, Wen-Quan Tao*

Key Laboratory of Thermo-Fluid Science and Engineering of MOE, School of Energy and Power Engineering, Xi'an Jiaotong University, Xi'an, Shaanxi 710049, China

HIGHLIGHTS

- Deviation of effective thermal conductivity via effective models is analyzed.
- An effective model based on the structures of aerogels is proposed and verified its adaptability.
- Thermal conductivity of two materials at different gas pressure is measured.
- Contribution of gas conduction, solid conduction and thermal radiation is decomposed.

ARTICLE INFO

Article history:
Received 30 September 2013
Accepted 20 February 2014
Available online 12 March 2014

Keywords:
Aerogels
Nano-porous material
Effective thermal conductivity
Effective model
Decomposition
Contribution

ABSTRACT

In this paper, a new effective model, spherical hollow cube model, is proposed based on the structures of aerogels and the prediction equation for the apparent thermal conductivity is theoretically derived. The effective thermal conductivity of different types of aerogels is estimated by the present model, and the predicted results are more agreeable with experimental data than that of the previous models. In addition, the thermal conductivity of two nano-porous materials at different gas pressure is investigated experimentally. The contributions of gas conduction, solid conduction and thermal radiation are obtained by decomposition method.

1. Introduction

Aerogels are typical nano-porous materials with open-cell structure manufactured through sol–gel process and supercritical drying technology [1,2]. The high porosity (85%–99%), large specific surface area (700–1300 m^2/g) and low density (3–150 kg/m^3) of aerogels result in their outstanding thermal insulation performance. The effective thermal conductivity of aerogels can reach as low as 0.012 W/m K [3] at ambient temperature and atmospheric pressure.

The heat transfer in aerogels includes collisions between gas molecules, gas convection in the pores, conduction through the solid skeleton and thermal radiation. However, gas convection could be neglected in porous materials when the pore size is less than 1 mm at ambient pressure [4]. Heat transfer in nano-porous materials has strong size effect for their nanoscale structure. The nano-porous skeleton restricts the motion of gas molecules and thus decreases the gaseous thermal conductivity [5]. The thermal resistance of the solid matrix is greater than that of the bulk materials with the same thickness due to the extremely long heat transfer path introduced by the porous structure. In addition, in aerogels the solid skeleton size is in the range of 2–5 nm, for which the phonon boundary scattering occupies a main part and lowers phonon mean free path greatly. Thereby, the thermal conductivity of solid skeleton is less than that of bulk materials. As far as the thermal radiation is concerned, plenty of heat shields are formed in aerogels which prevent the thermal radiation by reflection, adsorption, transmission and re-radiation at the numerous gas–solid interfaces. The difficulties of analyzing the effective thermal conductivity of aerogels also came from the fact that defects, opacifier and reinforced fibers with

* Corresponding author. Tel./fax: +86 029 82669106.
E-mail address: wqtao@mail.xjtu.edu.cn (W.Q. Tao).

http://dx.doi.org/10.1016/j.applthermaleng.2014.02.052
1359-4311/

micron size may exist in aerogels and its composites. All these complexities make the heat transfer in these materials multiscale in nature, i.e., heat transport phenomena in the aerogels include microscale, mesoscale and macroscale processes. Therefore, the effective thermal conductivity of aerogels and their composites depends on their microscale, mesoscale and macroscale structures, and the determination of their effective thermal conductivity is actually a multiscale problem [6].

For a fast engineering evaluation of the effective thermal conductivity, regular structures of aerogels are developed widely to replace the random structure in order to analyze the heat transfer characteristics and obtain some important average quantity. In the past two decades, many researchers proposed various effective models to estimate the effective thermal conductivity of porous materials. For example, Verma et al. [7] derived an expression for the prediction of effective thermal conductivity with spherical inclusions. Hsu et al. [8] developed a lumped-parameter model for the effective thermal conductivity of some two-dimensional and three-dimensional spatially periodic media. Gori et al. [9] used a cubic cell model to evaluate the thermal conductivity of an ablative composite material. Zeng et al. [10] proposed three effective models to calculate the thermal conductivity of pure aerogels. Although the thermal conductivity obtained from these models could fit well with experimental data qualitatively, how to improve quantitative agreement is still a big challenge and needs more theoretical and experimental studies.

As indicated above, the effective thermal conductivity of aerogel is composed of the contributions of gas conduction, solid conduction and thermal radiation. One way to understand the transmission mechanism in depth is to decompose the contributions of gas conduction, solid conduction and thermal radiation from the effective thermal conductivity and this will help to find the major heat transfer mechanism in aerogels and its composites. Some works have been conducted in this aspect [4,11,12], in which the gas pressure is lower than 1 bar.

In this paper, both theoretical and experimental studies are performed for the prediction of the effective thermal conductivity. Firstly, the reasons brought in the discrepancy of the effective thermal conductivity from different existing models are analyzed and a new effective model is proposed based on the structures of aerogels. The adaptability of the developed model is verified by comparing the predicted results with existing experimental data. Secondly, the transient plane source method is adopted to measure the effective thermal conductivity of some nano-porous materials. The Hot Disk thermal constant analyzer is combined with a molecular pump group, adjustable valves and a high pressure source to carry out the experiments at different gas pressure. The test range of gas pressure is extended to 1 MPa for thermal conductivity measurement of porous materials. The thermal conductivity of two nano-porous materials is measured at different gas pressure to decompose the contributions of gas heat conduction, solid heat conduction and thermal radiation.

In the following presentation, an improved model for the effective thermal conductivity is proposed based on the analyzing of the disadvantages of previous models in Section 2, then theoretical analysis is further made for gas, solid and radiative conductivity in Section 3. In Section 4 both theoretical and experimental results are presented and compared. Finally, some conclusions are presented in Section 5.

2. Effective thermal conductivity model of aerogel

2.1. Analyzing some previous effective models of aerogel

Zeng et al. [10] proposed intersecting square rod, intersecting cylindrical rod, and intersecting spherical structure as the simplified model for aerogel, with representative unit cells shown in Fig. 1. For the carbon-opacified aerogels (density 0.11 g/cm^3, porosity 0.94, specific surface area 797 m^2/g), the calculated effective thermal conductivity from the three models are 0.0419, 0.0414 and 0.0416 W/m K, respectively, which are nearly two times higher than the experimental value (0.0137 W/m K). The discrepancy in Zeng's analysis mentioned above is conjectured to be size effects to some extent. However, the intersecting spheres structure with the highest contact resistance (smallest contact ratio; i.e., $a/d = 0$) still results in a large predicted thermal conductivity of 0.0226 W/m K which is still higher than the experiment value, which indicates that other reasons also exist and have a significant influence.

According to the present authors' analysis, the discrepancy of the effective model is mainly introduced by the following reasons:

(1) The effective thermal conductivity derived from the models is based on the assumption of one dimension heat conduction while in fact three-dimension heat conduction occurs in aerogels as shown in the scanning electronic microscope image of silica aerogels in Fig. 2 by the present authors. Therefore, the effective thermal conductivity calculated from the effective model would be underestimated.
(2) Due to the random porous structure of aerogels, the actual solid heat transfer path of solid is much longer than that in the simplified periodic models. In this aspect, the thermal conductivity predicted by the effective model would be overestimated.
(3) The thermal conductivity of bulk materials was used as the thermal conductivity of solid skeleton. However, size effect exists in the solid skeleton of aerogels, so it is unreasonable

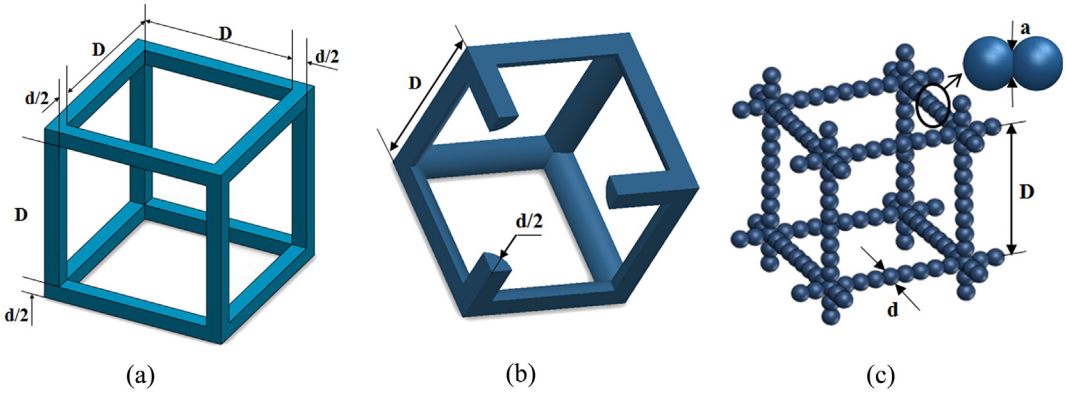

Fig. 1. Unit cells: (a) intersecting square rods; (b) intersecting cylindrical rods; (c) intersecting spheres.

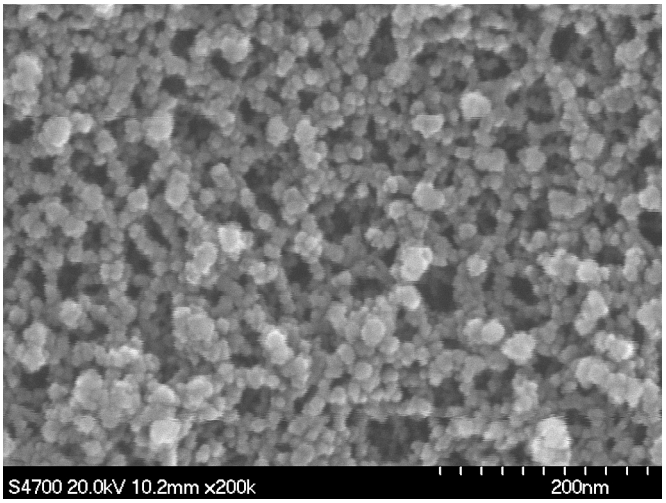

Fig. 2. Scanning electronic microscope images of aerogels.

to estimate the solid thermal conductivity in aerogels with the thermal conductivity of the bulk material [10,12]. When selecting the bulk thermal conductivity of solid to calculate, the predicted thermal conductivity will be too high.

(4) In some effective models, such as intersecting spheres model, the expression contains an empirical parameter which is usually determined through comparing with experiments case by case and thus it is lack of universality.

2.2. Proposal of an improved model – spherical hollow cube model

Song et al. [13] found that the solid structure of aerogels appears to be more fiber-like than particle-like estimated from the micrographs of aerogels; i.e., the intersecting square rods and the intersecting cylindrical rods should be closer to the real structure than the intersecting spheres. From the scanning electronic microscope images of aerogels as shown in Fig. 2, the interconnected pores occupy a majority of the material, and the solid material appears to be the support structure. Based on the structural property of aerogels, a new effective model is proposed by the present authors, spherical hollow cube model, as shown in Fig. 3.

For the spherical hollow cube model, 1/8 of the cube could be picked as a unit cell for the theoretical analysis, as shown in Fig. 4(a). Considering one dimension heat transfer assumption and assuming that heat transfers vertically from the bottom to the top of the unit cell, the effective conductivity calculated by such unit cell could be regarded as the conductivity of the macroscopic material. Heat transferred by conduction through the solid and gas can be decomposed into four parts, see Fig. 4(b), and their expressions derived by the present authors are as follows:

Q_1 is the heat transferred totally through solid skeleton:

$$Q_1 = \frac{\lambda_s A_1 \Delta T}{a/2} = \frac{\lambda_s \left[\frac{a^2-\pi r^2}{2} + 2\arccos\left(\frac{a}{2r}\right) r^2 - a\sqrt{r^2-\left(\frac{a}{2}\right)^2}\right]}{a}\Delta T \quad (1)$$

Q_2 is the heat transferred totally through the gas inside the unit cell:

$$Q_2 = \frac{\lambda_g A_2 \Delta T}{a/2} = \frac{\lambda_g \pi (r^2 - a^2/4)}{2a}\Delta T \quad (2)$$

where A_1 and A_2 are the heat transfer area.

Q_3 and Q_4 are the heat transferred through both gas and solid skeleton, as shown in Fig. 4(b). In the following, the two parts are calculated with integration method.

For Q_3, the following expression is derived:

$$Q_3 = \int_{\sqrt{r^2-a^2/4}}^{a/2} \frac{\frac{\pi}{2} x \mathrm{d}x \Delta T}{\sqrt{r^2-x^2}\Big/\lambda_g + \left(a/2 - \sqrt{r^2-x^2}\right)\Big/\lambda_s} \quad (3)$$

Substituting $x = r\sin\theta$, $r\sin\theta_1 = a/2$, $r\sin\theta_0 = \sqrt{r^2 - a^2/4}$ $\theta_1 = \arcsin(a/2r)$, and $\theta_0 = \arcsin(\sqrt{1-a^2/4r^2})$ into the above equation, the following expression is obtained.

$$\begin{aligned} Q_3 &= \int_{\theta_0}^{\theta_1} \frac{\frac{\pi}{2} r\sin\theta d(r\sin\theta)\Delta T}{r\cos\theta/\lambda_g + (a/2 - r\cos\theta)/\lambda_s} \\ &= -\frac{\lambda_s \pi \Delta T}{2k^2}\left[kr(\cos\theta_1 - \cos\theta_0) - \frac{a}{2}\ln\left(\frac{kr\cos\theta_1 + a/2}{kr\cos\theta_0 + a/2}\right)\right] \end{aligned} \quad (4)$$

where $k = \lambda_s/\lambda_g - 1$.

The expression for Q_4 can be derived as follows:

$$\begin{aligned} Q_4 &= \int_{a/2}^{r} \frac{\theta x \mathrm{d}x \Delta T}{\sqrt{r^2-x^2}\Big/\lambda_g + \left(a/2 - \sqrt{r^2-x^2}\right)\Big/\lambda_s} \\ &= \int_{a/2}^{r} \frac{2\arcsin\left(\frac{a/2-\sqrt{x^2-a^2/4}}{\sqrt{2}x}\right) x \mathrm{d}x \Delta T}{\sqrt{r^2-x^2}\Big/\lambda_g + \left(a/2 - \sqrt{r^2-x^2}\right)\Big/\lambda_s} \end{aligned} \quad (5)$$

where a is the side length of the cube, r is the radius of the spherical hollow, λ_s and λ_g are the thermal conductivity of solid

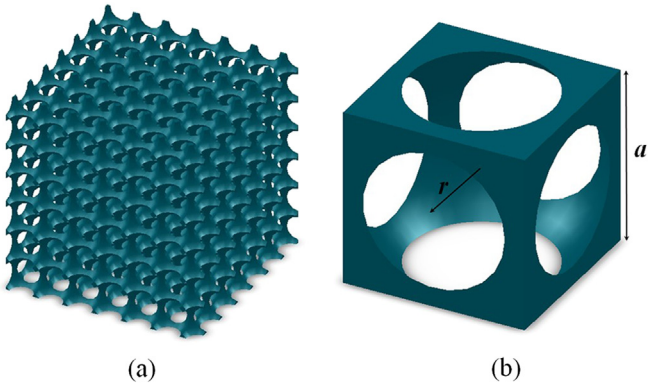

Fig. 3. Spherical hollow cube model: (a) overall viewing; (b) one spherical hollow cube.

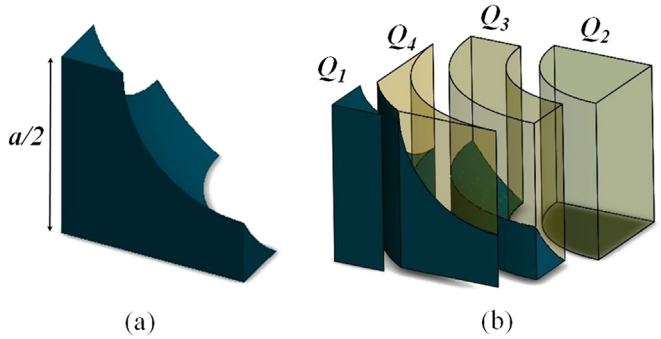

Fig. 4. Unit cell: (a) unit cell; (b) one dimension heat transfer.

and gas, respectively, and θ, θ_0, and θ_1 are intermediate variables for integration.

With the above derivations, the apparent conductivity due to conduction through gases and solid skeleton could be calculated as follows:

$$\lambda_c = \frac{Q_1+Q_2+Q_3+Q_4}{\Delta T\cdot a/2} = \frac{2\lambda_s\left[\frac{a^2-\pi r^2}{2}+2\arccos\left(\frac{a}{2r}\right)r^2-a\sqrt{r^2-\left(\frac{a}{2}\right)^2}\right]}{a^2}+\lambda_g\pi\left(\frac{r^2}{a^2}-\frac{1}{4}\right)-\frac{\lambda_s\pi}{k^2a}\left[kr(\cos\theta_1-\cos\theta_0)-\frac{a}{2}\ln\left(\frac{kr\cos\theta_1+a/2}{kr\cos\theta_0+a/2}\right)\right]+\frac{4}{a}\int_{a/2}^{r}\frac{\arcsin\left(\frac{a/2-\sqrt{x^2-a^2/4}}{\sqrt{2}x}\right)x\mathrm{d}x}{\sqrt{r^2-x^2}\Big/\lambda_g+\left(a/2-\sqrt{r^2-x^2}\right)\Big/\lambda_s} \quad (6)$$

The geometric parameters a and r are determined from the specific area S_s and the porosity Π. From the unit cell structure (Fig. 4), the specific surface area can be expressed as follows:

$$S_s = \frac{S}{m} = \frac{6\pi r}{\rho_{\mathrm{por}}a^2}-\frac{8\pi r^2}{\rho_{\mathrm{por}}a^3} \quad (7)$$

where, ρ_{por} is the density of aerogels and m is the mass of the unit cell.

The porosity can be determined by:

$$\Pi = -\frac{8\pi r^3}{3a^3}+\frac{3\pi r^2}{a^2}-\frac{\pi}{4} \quad (8)$$

With the specific surface area and porosity being determined, the geometric parameters a and r can be determined from Eqs. (7) and (8).

The specific surface area S_s and porosity Π can be measured through nitrogen adsorption and desorption measurements. In our calculation, the following relation is adopted to estimate the specific surface area of aerogels according to the measured and simulated results in literature [14–16]:

$$S_s = \left(342.3\Big/\rho_{\mathrm{por}}+5.03\right)\times 10^5 \quad (9)$$

Porosity of aerogels can be estimated with formula $\Pi = 1-\rho_{\mathrm{por}}/\rho_{\mathrm{bulk}}$, where ρ_{bulk} is the density of solid skeleton which can be measured through experimental methods. In this paper, a skeleton density of 2200 kg/m^3 is adopted for the calculation.

Fig. 5 illustrates the variations of a and r with the aerogels density. It is shown that both a and r decrease with the increase of the density of aerogel. As both the radius of the spherical hollow r and the side length of the unit cell a are in the range from several to a dozen nanometers, which are agreeable with statistic data of aerogels, it implies that the spherical hollow cube model is a reasonable representation of aerogels.

It should be noted here that Eq. (6) gives the contributions of gases and skeleton, and this equation is an expression for gas–solid coupled conduction, without the radiative contribution. In the next section, some theoretical results for gas, skeleton and radiation contributions will be provided.

3. Theoretical analysis for gas, solid and radiative conductivity

The above discussion reveals that the effective thermal conductivity of nano-porous materials can be recognized as the sum of contributions from several parts: heat conduction through the gas, $\lambda_{g,0}$, heat conduction through the solid, $\lambda_{s,0}$, and radiation through the skeleton and voids, $\lambda_{r,0}$. In nano-porous materials, heat transfers via the solid skeleton and the gas molecules continually. It is a coupled process. However, the heat transfer through radiation could be superposed with the coupled heat conduction directly. So the effective thermal conductivity of nano-porous materials can also be recognized as a sum of λ_c and λ_r, where λ_c is a combination of solid thermal conductivity, λ_s, and gas thermal conductivity, λ_g. It is noted that λ_c is correlated with the porosity and the space structure of a material.

$$\lambda_e = \lambda_{s,0}+\lambda_{g,0}+\lambda_{r,0} = \lambda_c+\lambda_r \quad (10)$$

where λ_{s0}, λ_{g0}, λ_{r0} represent the contributions of solid, gas and radiation, respectively, to the thermal conductivity of aerogels.

3.1. Solid thermal conductivity

As indicated above, due to the size effect, the thermal conductivity of solid skeleton of nano-porous materials is different from the corresponding bulk materials. Reference [17] gives the following equation for the thermal conductivity of solid skeleton:

$$\lambda_s = \lambda_{s,s}\frac{\rho\nu}{\rho_s\nu_s} \quad (11)$$

where, $\lambda_{s,s}$ is the thermal conductivity of the bulk material, ρ and ρ_s are the densities of the porous material and solid skeleton, ν and ν_s are the longitudinal sound velocities of the porous materials and the bulk materials.

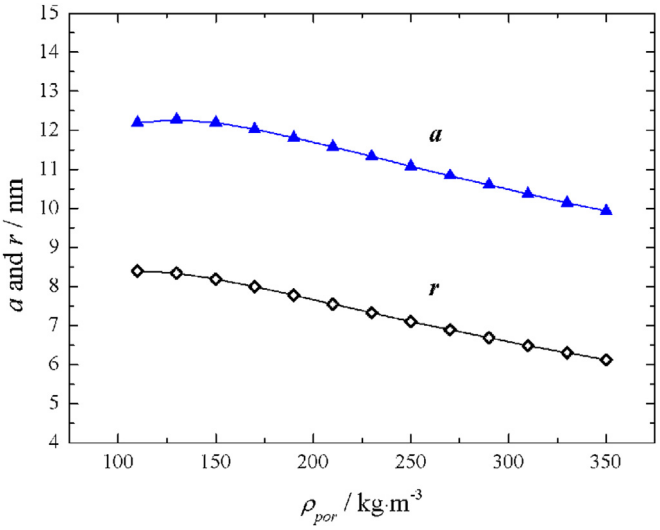

Fig. 5. Variations of a and r with aerogel porosity.

Hrubesh and Pekala [18] proposed the approximate formulas for the sound velocities of different materials.

3.2. Gas thermal conductivity

Typically, nano-porous materials such as aerogels have pore sizes on the magnitude of 10 nm, which is less than the mean free path of gas (70 nm for air) in free space at normal pressure and temperature. Therefore, the motion of gas molecules in porous medium is suppressed by the porous framework and the gas thermal conductivity within nano pores is lower than that in free space. The gas thermal conductivity between two parallel plates was presented by Kaganer [19]:

$$\lambda_g = \lambda_g^0 \Big/ \left(1 + 2\frac{2\gamma}{\gamma+1}\frac{1}{Pr}\frac{2-\alpha}{\alpha}Kn\right) \tag{12}$$

where, λ_g^0 is the gas thermal conductivity in free space, $\gamma = c_p/c_v$, c_p and c_v are the specific heat at constant pressure and volume respectively, Pr is the Prandtl number, α is the accommodation coefficient, $Kn = l_m/l_{ch}$ is the Knudsen number, l_{ch} is the distance between the plates, and l_m is the mean free path of gas molecules.

The mean free pass of gas molecules in free space is calculated as:

$$l_m^0 = \frac{1}{\sqrt{2}n_g\pi d_g^2} = \frac{k_B T}{\sqrt{2}p\pi d_g^2} \tag{13}$$

where n_g is the number density of gas molecules, d_g is the diameter of the gas molecules, k_B is the Boltzmann constant, and p and T are gas pressure and temperature.

However, the mean free path of gas molecules is greatly reduced as the motion of gas molecules in aerogels is largely restricted by the nanoscale porous framework. Zeng et al. [20] derived the mean free path of gas molecules in porous medium based on the kinetic theory:

$$l_m = \frac{1}{\sqrt{2}n_g\pi d_g^2 + 0.25S_s\rho_{por}\Big/\Pi} \tag{14}$$

where $0.25S_s\rho/\Pi$ represents the part of mean free path restricted by the solid skeleton.

The gas thermal conductivity in free space based on the kinetic theory was derived by Loeb [21]:

$$\begin{aligned}\lambda_g^0 &= (2.25\gamma - 1.25)\eta c_v \\ &= (2.25\gamma - 1.25)0.461 n_g m_g \left(8k_B T/\pi m_g\right)^{1/2} l_m C_v/N_A m_g)\end{aligned} \tag{15}$$

where η is the viscosity of gas determined by:

$$\eta = 0.461 n_g m_g \left(8k_B T/\pi m_g\right)^{1/2} l_m \tag{16}$$

Substituting Eqs. (14)–(16) into Eq. (12), the gas thermal conductivity in a porous medium could be derived [22,23].

$$\lambda_g = \frac{\dfrac{(2.25\gamma-1.25)0.461(p/k_BT)\left(8k_BT/\pi m_g\right)^{1/2} m_g c_v}{0.25S_s\rho_{por}\Pi^{-1}+\sqrt{2}(p/k_BT)\pi d_g^2}}{1 + 2\dfrac{2\gamma}{\gamma+1}\dfrac{1}{Pr}\dfrac{2-\alpha}{\alpha}\dfrac{1}{\sqrt{2}\pi d_g^2 p\Big/k_BT + 0.25S_s\rho_{por}\Pi^{-1}}\dfrac{1}{l_{ch}}} \tag{17}$$

where, m_g is the mass of gas molecules, S_s is the specific surface area, ρ_{por} is the apparent density of the porous medium, Π is the porosity of the porous medium, and d_g is the diameter of the gas molecules.

3.3. Radiative thermal conductivity

In practical application, the optical thickness of nano-porous materials is typically very large. Therefore, according to the Rossland diffusion approximation, the radiative thermal conductivity can be described as follows [24]:

$$\lambda_r = \frac{16n^2\sigma T^3}{3\rho_{por}K_{e,m}} \tag{18}$$

where σ is the Stefan–Boltzmann constant, n is the mean refractive index, T is the absolute temperature, ρ_{por} is the density of nano-porous materials and $K_{e,m}$ is the specific extinction coefficient.

It worth noting that Eqs. (11), (12) and (18) present the absolute thermal conductivity when the three heat transfer modes exist individually. Except the radiative conductivity (for which $\lambda_r = \lambda_{r,0}$), λ_s, λ_g determined by Eqs. (11) and (12) are different from $\lambda_{g,0}$, $\lambda_{s,0}$ in Eq. (10). Because of the collisions between gaseous molecules and the solid skeleton the gaseous conductive contributions, $\lambda_{g,0}$, may be higher than λ_g. On the other side, the contribution of solid, $\lambda_{s,0}$, is different from the solid conductivity obviously.

4. Results and discussion

4.1. Adaptability of the proposed spherical hollow cube model

Table 1 shows the comparison between thermal conductivity predicted by Zeng's three models (Zeng 1: intersecting square rods; Zeng 2: intersecting cylindrical rods; Zeng 3: intersecting spheres) and the existing experimental data [10,12,25].

The conductivity of bulk material (λ_s = 1.34 W/m K) is firstly used as solid thermal conductivity for the calculation of the total effective thermal conductivity. It is noticed that the effective thermal conductivity calculated with the three models are nearly two times higher than the experimental values [10,12,25]. The thermal conductivity of solid skeleton is then revised in order to match with the experimental results, as shown in the right half of the table.

It is also worth noting that for the intersecting square rod model and intersecting cylindrical rod model, there are no empirical parameters; however for the intersecting spheres structure, there exists an empirical parameter, a/d, which needs to be assumed artificially for the calculation of the effective thermal conductivity. The fitted solid thermal conductivities of different models and parameters are different, which proves that the fitted solid thermal conductivity lacks of universality.

The adaptability of the spherical hollow cube model is shown in Table 2. For this model, no parameter needs to be assumed and the coupled thermal conductivity of conduction is directly calculated with Eq. (6). The conductivity of bulk material (1.34 W/m K) is adopted for the solid conductivity. The effective thermal conductivity predicted by the model could fit well with experiment data with a maximum deviation of 30%. The deviation comes from the determinations of specific area and the experimentally-measured thermal conductivity, as well as the simplification of model. However, the comparison proves that the proposed model could be used to predict the effective thermal conductivity of aerogels with an accuracy acceptable by engineering calculation.

4.2. Decomposition of thermal conductivity

Transient plane source (TPS) method is a well-suited and accurate method for measuring thermal conductivity and diffusivity of materials [26]. In this work, experimental apparatus based on the TPS method is adopted to study the influences of temperature, gas

Table 1
Adaptability of Zeng's models and revision of solid conductivity.

ρ_{por} (g/cm^3)	S_s (m^2/g)	Experiment (W/m K)	Effective models (W/m K)			Revised solid conductivity (W/m K)			
			Zeng1	Zeng2	Zeng3 ($a/d = 0.1$)	Zeng1	Zeng2	Zeng3 ($a/d = 0.1$)	Zeng3 ($a/d = 0.2$)
0.098	833.0	0.0126	0.0330	0.0330	0.0140	0.15	0.14	0.11	0.11
0.110	797.6	0.0137	0.0355	0.0394	0.0150	0.21	0.18	0.29	0.23
0.114	787.5	0.0142	0.0363	0.0363	0.0146	0.23	0.22	0.81	0.54
0.126	760.4	0.0154	0.0389	0.0389	0.0150	0.28	0.27	1. 70	1.11
0.185	678.3	0.0191	0.0534	0.0523	0.0170	0.35	0.35	3.52	1.43
0.239	638.7	0.0229	0.0656	0.0656	0.0213	0.36	0.36	4.90	1.81

Table 2
Adaptability of the developed model.

ρ_{por} (g/cm^3)	S_s (m^2/g)	Experiment (W/m K)	New model (W/m K)	Deviation (%)
0.098	833.9	0.0126	0.0114	9.52
0.110	797.6	0.0137	0.0118	13.87
0.114	787.4	0.0142	0.0126	29.66
0.126	760.4	0.0154	0.0135	28.29
0.185	678.3	0.0191	0.0203	6.65
0.239	638.7	0.0229	0.0291	27.46

pressure and atmosphere on the effective thermal conductivity of nano-porous materials simultaneously. The experimental apparatus is shown in Fig. 6. The system contains a hot disk thermal constant analyzer (type: TPS2500S), a tube heating furnace, a temperature control system, a pressure gage, molecular pump systems, a high pressure source of inert gas and adjustable valves. The gas pressure range is from 0.01 Pa to 1 MPa. The accuracy of the apparatus is validated by NIST1453 standard sample, an expanded polystyrene board with thermal conductivity 0.032 W m^{-1} K^{-1} at room temperature and the deviation is within ±1.5%. The effective thermal conductivity of nano-porous material at different gas pressure is measured by the following procedures. Firstly, place the sample and sensor in the tube furnace as shown in Fig. 6. Secondly, pump the tube furnace with molecular pump group system until the gas pressure bellow 0.01 Pa to exclude the adsorbed gas or water completely and then filled with nitrogen to constant pressure. The pumping will be conducted for 3 times and then using the adjustable valve and gas source to reach the target pressure. Finally, the thermal conductivity measurement is conducted more than 3 times to obtain their mean value. The thermal conductivity measurement at different gas pressure should be conducted from low gas pressure to high gas pressure to avoid the adsorption and desorption hysteresis.

Two nano-porous materials, material a (apparent density = 594 kg/m^3, porosity = 71.8%) and material b (Super-G, apparent density = 240 kg/m^3, porosity = 89%) are experimentally investigated. The experiment is conducted within a gas pressure from 0.01 Pa to 1 MPa in nitrogen atmosphere at 297 K and the

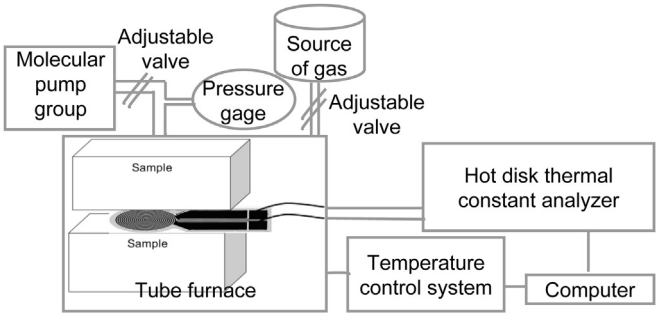

Fig. 6. Schematic illustration of the experimental apparatus.

effective thermal conductivity is shown in Fig. 7. The effective thermal conductivity of the two materials varies greatly with gas pressure. When the gas pressure is less than 0.01 kPa, the effective thermal conductivity remains a constant, which implies that gas heat conduction could be neglected here and it is the total contributions of solid conduction and thermal radiation.

The radiative thermal conductivity, λ_r, could be calculated from Eq. (18) with refractive index, $n = 1$ and $K_{e,m} = 50$ m^2/kg [4]. The contribution of solid heat conduction to the effective thermal conductivity, $\lambda_{s,0}$, can be obtained by subtracting radiative thermal conductivity from the effective thermal conductivity at low gas pressure where the contribution of gas heat conduction is negligible. Finally, the contribution of gas heat conduction, $\lambda_{g,0}$, can be obtained by subtracting $\lambda_{s,0}$ and λ_r from the total thermal conductivity measured at different gas pressure. The decomposed contributions of gas heat conduction, solid heat conduction and thermal radiation of the two materials at 297 K are shown in Fig. 7(a) and (b), respectively. It is noted that thermal radiation, λ_r, gives little contribution to the total thermal conductivity at ambient temperature. For material a, the contribution of solid heat conduction is always higher than that of gas conduction; while for material b, Super-G, the contribution of solid heat conduction, $\lambda_{s,0}$, dominates when the gas pressure is less than 20 kPa and the influence of gas pressure play a dominant role when the pressure is higher than 20 kPa.

4.3. Contribution of gas heat conduction

The decomposed contribution of gas heat conduction from the experimental results is used to compare with the absolute gas conductivity in nano-porous materials and the gas conductivity in free space, as illustrated in Fig. 8.

In free space, the gas heat conduction could be neglected when the pressure is less than 0.1 Pa, then it increases with gas pressure and closes to constant when the pressure is higher than 1 kPa. In nano-porous materials, however, the gas thermal conductivity could be neglected when the gas pressure is less than 1 kPa, and it still does not reach the maximum value and less than that in free space at 1 MPa.

The contribution of gas heat conduction has the same variation tendency with the gas thermal conductivity. The contribution of gas heat conduction is higher than the gas thermal conductivity when the gas thermal conductivity could be distinguished. Both the contribution of gas conduction and the gas conductivity rapidly increase when the pressure is higher than 0.1 kPa. The higher the pressure, the greater difference between the two curves. The decomposed contribution of gas heat conduction, $\lambda_{g,0}$, is even higher than the gas thermal conductivity in free space at high gas pressure. For example, $\lambda_{g,0}$ at 1 MPa (0.034 W/m K) is higher than the thermal conductivity of free nitrogen (0.026 W/m K), as shown in the figure. The contribution of gas heat conduction is influenced not only by gas thermal conductivity in nano-porous materials, but also by the skeleton thermal conductivity, porosity and the microstructure as well.

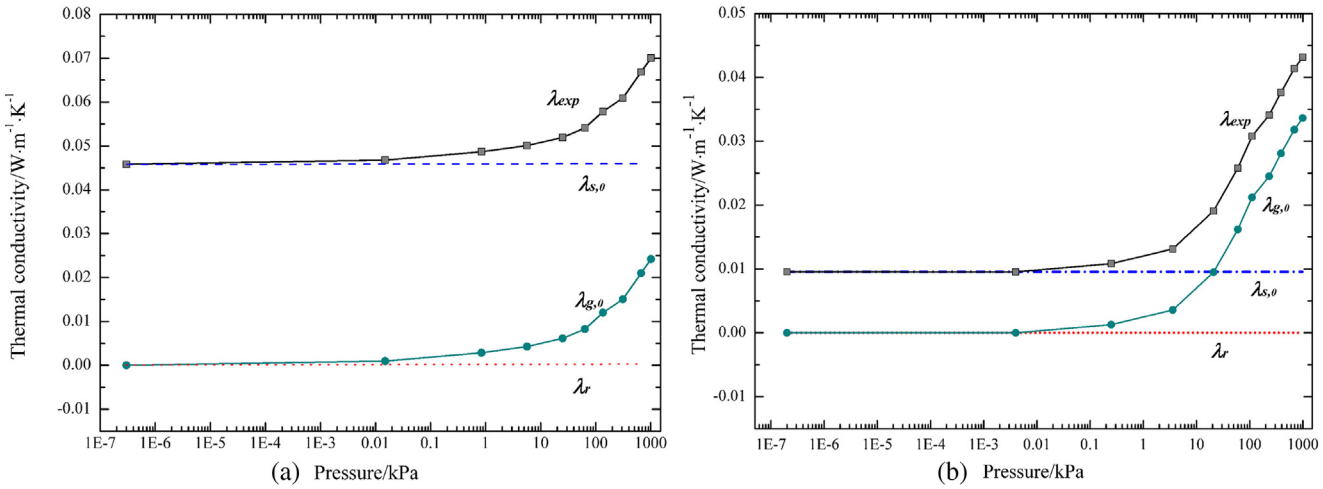

Fig. 7. Decomposition of the effective thermal conductivity: (a) Material a, por = 71.8%; (b) Material b, por = 89%.

As shown in Eqs. (15) and (16), the gas thermal conductivity is proportional to the number density of gas molecules and the mean free path. The number density of gas molecules increases linearly with pressure while the variations of the mean free path in free space and nano-porous materials are different. The mean free paths in free space and nano-porous materials are shown in Fig. 9. The mean free path in free space decreases linearly with the increase of pressure in log–log coordinate. However, the mean free path in nano-porous materials remains constant when the pressure is less than 100 kPa, then the mean free path decreases and closes to the value in free space gradually when the pressure is higher than 100 kPa. Such difference is caused by the suppressed motion of gas molecules in nano-porous materials, which introduces the apparent difference of gas thermal conductivity in nano-porous materials from that in free space.

5. Conclusion

In this work, the reasons accounting for the appreciable deviation of effective thermal conductivity predicted by previous effective models such as Zeng's models are analyzed comprehensively. A spherical hollow cube model is proposed based on the structures of aerogels. Compared with the existing theoretical models, the present model does not need any empirical parameters and it is thus a suitable representation for aerogels. The deviation between the conductivity predicted by model and experimental results is greatly improved compared with previous models and it could meet the needs for fast prediction in engineering.

The thermal conductivity of two materials is measured within gas pressure ranged from 0.01 Pa to 1 MPa. The contributions of gas heat conduction, solid heat conduction and thermal radiation to the effective thermal conductivity are decomposed from the effective thermal conductivity. The contribution of gas heat conduction has a great influence on the effective thermal conductivity of nano-porous materials and is appreciably higher than the gas thermal conductivity in nano-porous materials. Filling materials with low thermal conductivity gas, as well as using them under the environment of a certain vacuum could improve the thermal insulation property of aerogels and its composites.

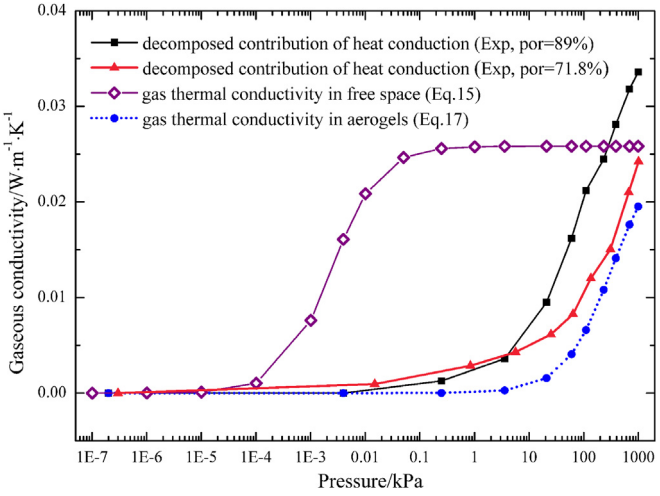

Fig. 8. Contribution of gas heat conduction.

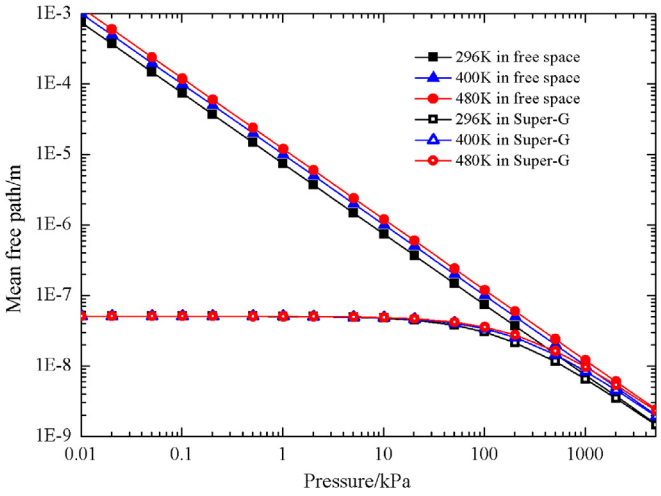

Fig. 9. Mean free path of nitrogen molecules.

Acknowledgements

The authors would like to thank the supports from National Natural Science Foundation of China (Grant number 51320105004 and 51276138).

References

[1] X. Lu, M.C. Arduinischuster, J. Kuhn, O. Nilsson, J. Fricke, R.W. Pekala, Thermal-conductivity of monolithic organic aerogels, Science 255 (1992) 971–972.
[2] M. Schmidt, F. Schwertfeger, Applications for silica aerogel products, J. Non-Cryst. Solids 225 (1998) 364–368.
[3] M. Wang, N. Pan, Predictions of effective physical properties of complex multiphase materials, Mater. Sci. Eng. R 63 (2008) 1–30.
[4] O.J. Lee, K.H. Lee, T.J. Yim, S.Y. Kim, K.P. Yoo, Determination of mesopore size of aerogels from thermal conductivity measurements, J. Non-Cryst. Solids 298 (2002) 287–292.
[5] J.L. Gurav, A.V. Rao, D.Y. Nadargi, Study of thermal conductivity and effect of humidity on HMDZ modified TEOS based aerogel dried at ambient pressure, J. Sol-Gel Sci. Technol. 50 (2009) 275–280.
[6] Y.L. He, W.Q. Tao, Multiscale simulations of heat transfer and fluid flow problems, ASME J. Heat Transfer 134 (2012) 1–13.
[7] L.S. Verma, A.K. Shrotriya, R. Singh, D.R. Chaudhary, Thermal conduction in two-phase materials with spherical and nonspherical inclusions, J. Phys. D-Appl. Phys. 24 (1991) 1729–1737.
[8] C.T. Hsu, P. Cheng, K.W. Wong, A lumped-parameter model for stagnant thermal conductivity of spatially periodic porous media, Trans. ASME J. Heat Transfer 117 (1995) 264–269.
[9] F. Gori, S. Corasaniti, W.M. Worek, W.J. Minkowycz, Theoretical prediction of thermal conductivity for thermal protection systems, Appl. Therm. Eng. 49 (2012) 124–130.
[10] S.Q. Zeng, A. Hunt, R. Greif, Geometric structure and thermal conductivity of porous medium silica aerogel, Trans. ASME J. Heat Transfer 117 (1995) 1055–1058.
[11] G. Lu, X.D. Wang, Y.Y. Duan, X.W. Li, Effects of non-ideal structures and high temperatures on the insulation properties of aerogel-based composite materials, J. Non-Cryst. Solids 357 (2011) 3822–3829.
[12] G.S. Wei, Y.S. Liu, X.X. Zhang, D.Y. Liu, Thermal conductivity measurement on silica aerogel and its composite insulation materials, J. Eng. Thermophys. 32 (2011) 667–670.
[13] X.Y. Song, W. Cao, A.J. Hunt, Aem and hrem evaluation of carbon nano-structures in silica aerogels, in: MRS Spring Meeting, vol. 349, 1994, pp. 269–274. San Francisco, CA.
[14] P.I. Pohl, J.L. Faulon, D.M. Smith, Molecular-dynamics computer-simulations of silica aerogels, J. Non-Cryst. Solids 186 (1995) 349–355.
[15] G. Biesmans, D. Randall, E. Francais, M. Perrut, Polyurethane-based organic aerogels' thermal performance, J. Non-Cryst. Solids 225 (1998) 36–40.
[16] H.L. Zhang, J. Wang, Z.S. Deng, B. Zhou, Gas thermal conduction of nano-porous silica aerogels, J. Tongji Univ. 27 (1999) 541–544.
[17] R. Berman, Thermal Conduction in Solids, Clarendon Press, 1976.
[18] L.W. Hrubesh, R.W. Pekala, Thermal properties of organic and inorganic aerogels, J. Mater. Res. 9 (1994) 731–738.
[19] M.G. Kaganer, Thermal Insulation in Cryogenic Engineering, Israel Program for Scientific Translations, 1969.
[20] S.Q. Zeng, A. Hunt, R. Greif, Mean free path and apparent thermal conductivity of a gas in a porous medium, J. Heat Transfer 117 (1995) 758–761.
[21] L.B. Loeb, The Kinetic Theory of Gases, McGraw-Hill, New York, 1934.
[22] S.Q. Zeng, A. Hunt, R. Greif, Transport properties of gas in silica aerogel, J. Non-Cryst. Solids 186 (1995) 264–270.
[23] H. Zhang, Z.Y. Li, D. Dan, W.Q. Tao, The influence of gas pressure on the effective thermal conductivity of nano-porous material, J. Eng. Thermophys. 34 (2013) 1–4.
[24] R. Siegel, J. Howell, Thermal Radiation Heat Transfer, New York London, fourth ed., 2002.
[25] X. Lu, R. Caps, J. Fricke, C.T. Alviso, R.W. Pekala, Correlation between structure and thermal-conductivity of organic aerogels, J. Non-Cryst. Solids 188 (1995) 226–234.
[26] S.A. Al-Ajlan, Measurements of thermal properties of insulation materials by using transient plane source technique, Appl. Therm. Eng. 26 (2006) 2184–2191.